

## Experimental Analysis of Aerodynamic Forces for Cross Flow on Single Rectangular Cylinder

A.M.Tito Islam\*  
A.C.Mandal\*

### ABSTRACT

An experimental investigation of static pressure distributions on rectangular cylinders for a uniform cross flow is performed. The effect of side ratios and angle of attack are encountered in the investigation. Drag and lift coefficients are presented which are calculated from measured pressure distributions.

### NOMENCLATURE

A	Area
$C_D$	Drag coefficient
$C_L$	Lift coefficient
$C_p$	Pressure coefficient
D	Width of Cylinder
$F_D$	Drag Force
$F_L$	Lift Force
H	Breadth of Cylinder
H/D	Side Ratio of Cylinder
$L_l$	Longitudinal Spacing
$L_t$	Transverse Spacing
P	Local Static Pressure
$P_o$	Free Stream Static Pressure
$U_o$	Free Stream Velocity
$\alpha$	Angle of Attack
$\rho$	Density of air

### INTRODUCTION

Engineering problems regarding wind loads around skyscrapers, chimneys, towers and the flow induced vibrations of tubes in heat exchangers, bridges, oil rigs or marine structures need detailed investigation of flow patterns and aerodynamic characteristics on bluff bodies. In the case of flow over a bluff body the separation points are fixed at the leading edges and the shear layers originating from the leading corners curve outwards and a wake region is formed behind the body.

Till now extensive research work has been carried out on flow over isolated bluff bodies. P.W.Bearman and D.M.Trueeman (1972) investigated the base pressure coefficient, drag coefficient and Strouhal number of rectangular cylinders. Y.Nakamura and Yujiohya (1986) attempted to study vortex shedding from square prisms placed normal to smooth and turbulent approach flows. B.E.Lee(1975) made an elaborate

study of the effect of turbulence on the surface pressure field of a square prism. A.R.Barriga, C.T.Crowe and J.A.Roberson (1975) studied the effects of angle of attack, turbulence intensity and scale on the pressure distribution of a single cylinder.

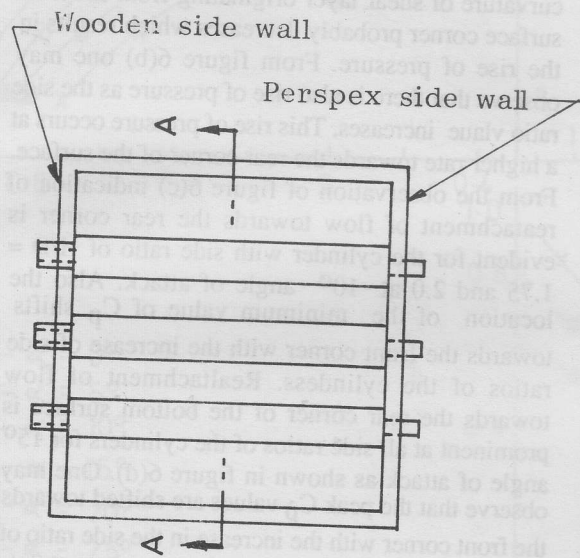
Rectangular cylinders ideally represent the general shape of tall buildings. So wind tunnel experiments on rectangular cylinders would be useful in the analysis of wind effects on tall buildings. The present experimental investigation is an attempt to make an understanding of the nature of mean pressure distributions and drag on rectangular cylinders with varying side ratios (ratio of breadth H to width D of the cross section of cylinder). The experiment is conducted for a uniform cross flow. The flow direction is varied in order to determine the effect of angle of attack on pressure distribution. The present experimental results are compared with the existing ones.

### EXPERIMENTAL SET UP AND PROCEDURE

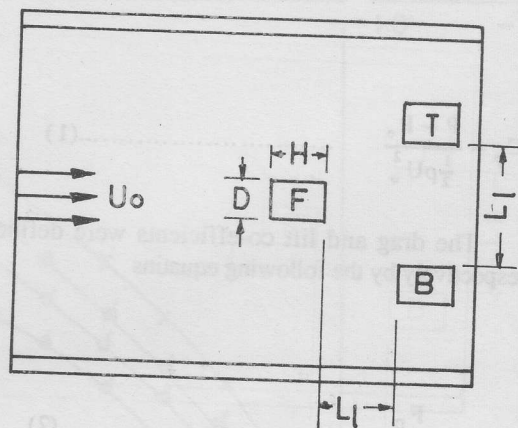
The experiment was carried out in an open circuit subsonic wind tunnel with a test section of 457mm X 457mm (18 inch X 18 inch) cross section. Four rectangular cylinders were used. The cylinders spanned 457mm each and their side dimensions were: width  $D=30\text{mm}$  for each, breadth  $H=37.5\text{mm}$ ,  $45\text{mm}$ ,  $52.5\text{mm}$  and  $60\text{mm}$ . Each rectangular cylinder was tapped on two adjacent sides to measure pressure distribution. Flexible tubes of 1.6mm outer diameter were used to connect the tappings to the limbs of a multimanometer. Water was used as the manometric fluid.

The rectangular cylinder of side ratio  $H/D= 1.25$

\* Mechanical Engineering Department, BUET, Dhaka



End view of test section



A-A Section

Figure 1: Tunnel Test Section showing the position of cylinders in staggered form.



was mounted centrally in a horizontal plane in the test section so that the 30mm face was oriented normal to the flow direction (Fig. 1). For angular orientation of the cylinders a graduated disc was used. Mean pressure distribution was recorded at angles of attack varying from 0° to 45° with a step of 5°.

Pressure distributions for each of the cylinders with side ratio of 1.25, 1.5, 1.75 and 2.0 were measured in a similar manner.

The flow velocity in the test section was kept constant at 18.3 m/s (60fps). The Reynolds number based on the side dimension  $D=30\text{mm}$  was  $3.45 \times 10^4$ . the turbulence intensity of the tunnel was approximately 0.33%.

The pressure co-efficient is defined as

$$C_p = \frac{P - P_o}{\frac{1}{2}\rho U_o^2} \dots\dots\dots(1)$$

The drag and lift co-efficients were defined respectively by the following equatins

$$C_D = \frac{F_D}{\frac{1}{2}\rho A U_o^2} \dots\dots\dots(2)$$

$$C_L = \frac{F_L}{\frac{1}{2}\rho A U_o^2} \dots\dots\dots(3)$$

The  $C_p$ ,  $C_D$  and  $C_L$  values were determined by numerical integration using Simpson's Rule.

## RESULTS AND DISCUSSIONS

Figures 2 to 5 show the effect of angle of attack on mean pressure co-efficients around the rectangular cylinders for side ratios of  $H/D = 1.25, 1.5, 1.75$  and  $2.0$  respectively. It is observed from

these figures that the overall patterns of the  $C_p$ -distribution curves for all the rectangular bodies on all the four surfaces are almost similar. However, remarkable variations in  $C_p$ -distributions is observed on the windward side (bottom surface) of each cylinder at small angle angle of attack due to change in side dimension. The effect of side ratios on the  $C_p$ -distributions for windward side of the rectangular cylinders at angles of attack of 0°, 5°, 10°, 15°, and 30° are shown in figure 6. It is clearly seen from the figure 6(a) that there is rise in pressure with the increase in the side ratio ( $H/D$ ) of rectangular cylinders at 0° angle of attack. Due to the increase of side ratio of the cylinder, the curvature of shear layer originating from the front surface corner probably decreases which results in the rise of pressure. From figure 6(b) one may observe that there is also rise of pressure as the side ratio vlaue increases. This rise of pressure occurs at a higher rate towards the rear corner of the surface. From the observation of figure 6(c) indication of reattachment of flow towards the rear corner is evident for the cylinder with side ratio of  $H/D = 1.75$  and  $2.0$  at 10° angle of attack. Also the location of the minimum value of  $C_p$  shifts towards the front corner with the increase of side ratios of the cylindess. Realtachment of flow towards the rear corner of the bottom surface is prominent at all side ratios of the cylinders for 15° angle of attack as shown in figure 6(d). One may observe that the peak  $C_p$  values are shifted towards the front corner with the increase in the side ratio of the rectangular cylinders. At 30° angle of attack it is seen that for side ratio of  $H/D = 1.75$  and  $2.0$  the peak  $C_p$  value is almost at the front corner suggesting separated flow.

The effect of side ratios on  $C_p$  distributions on the back surface of cylinder at angles of attack of 0°, 10°, 20°, 30° and 45° are shown in figure 7. It is seen that at 0° angle of attack (figure 7a) minimum  $C_p$  values exists for side ratio  $H/D = 1.25$  and it rises with the increase in side ratio. But with the increase in angle of attack as the figure reveals  $C_p$  values diminishes and at angle of attack of 45° (figure 7e) lowest  $C_p$  values occur for side ratio of  $H/D = 2.0$ . However, from figure 7d it can be observed that at 30° angle of attack the  $C_p$  distributions for all side ratios are very close.

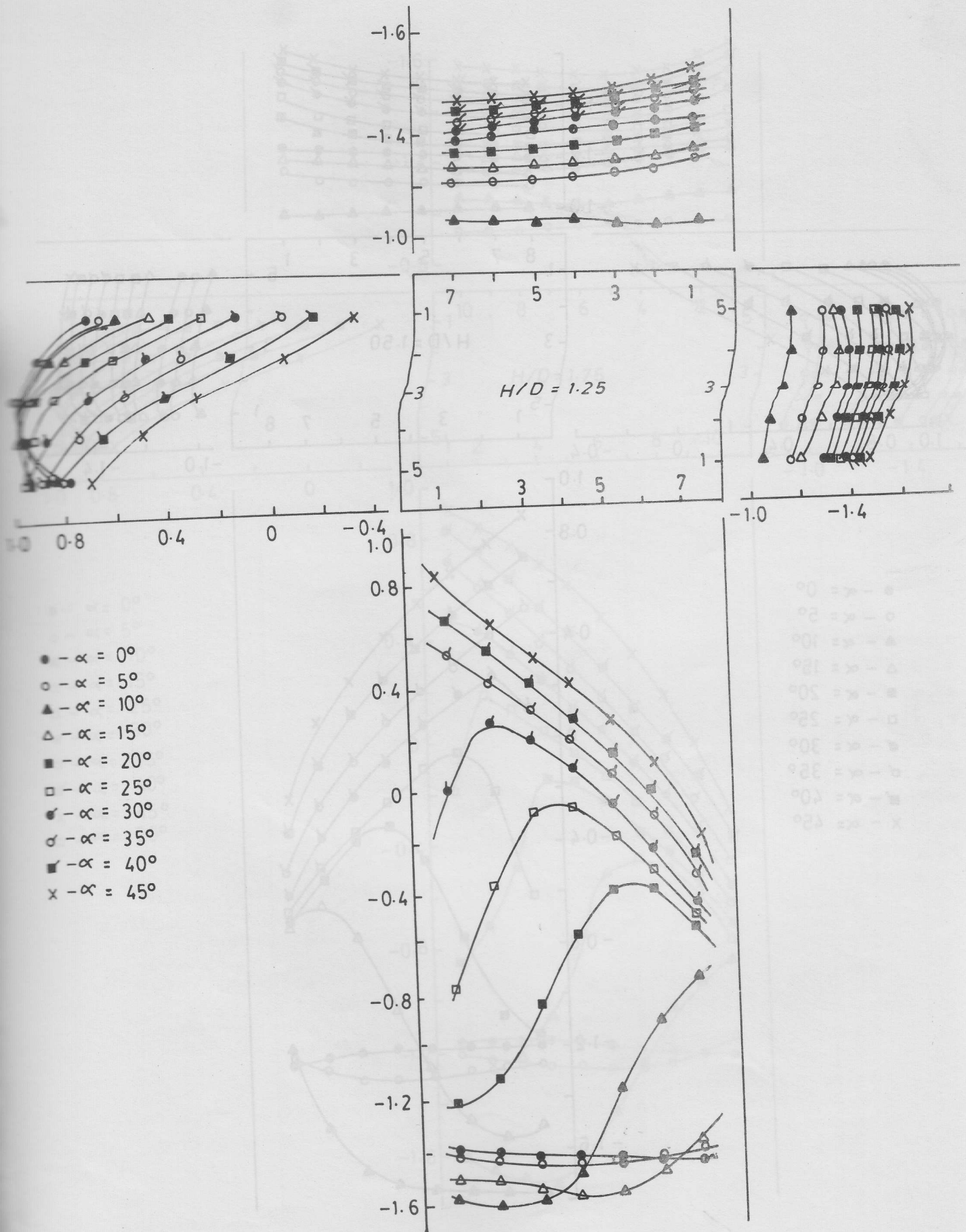


Figure 2: Effect of angle attack ( $\alpha$ ) on  $C_p$ -distribution at side ratio ( $H/D$ ) of 1.25.

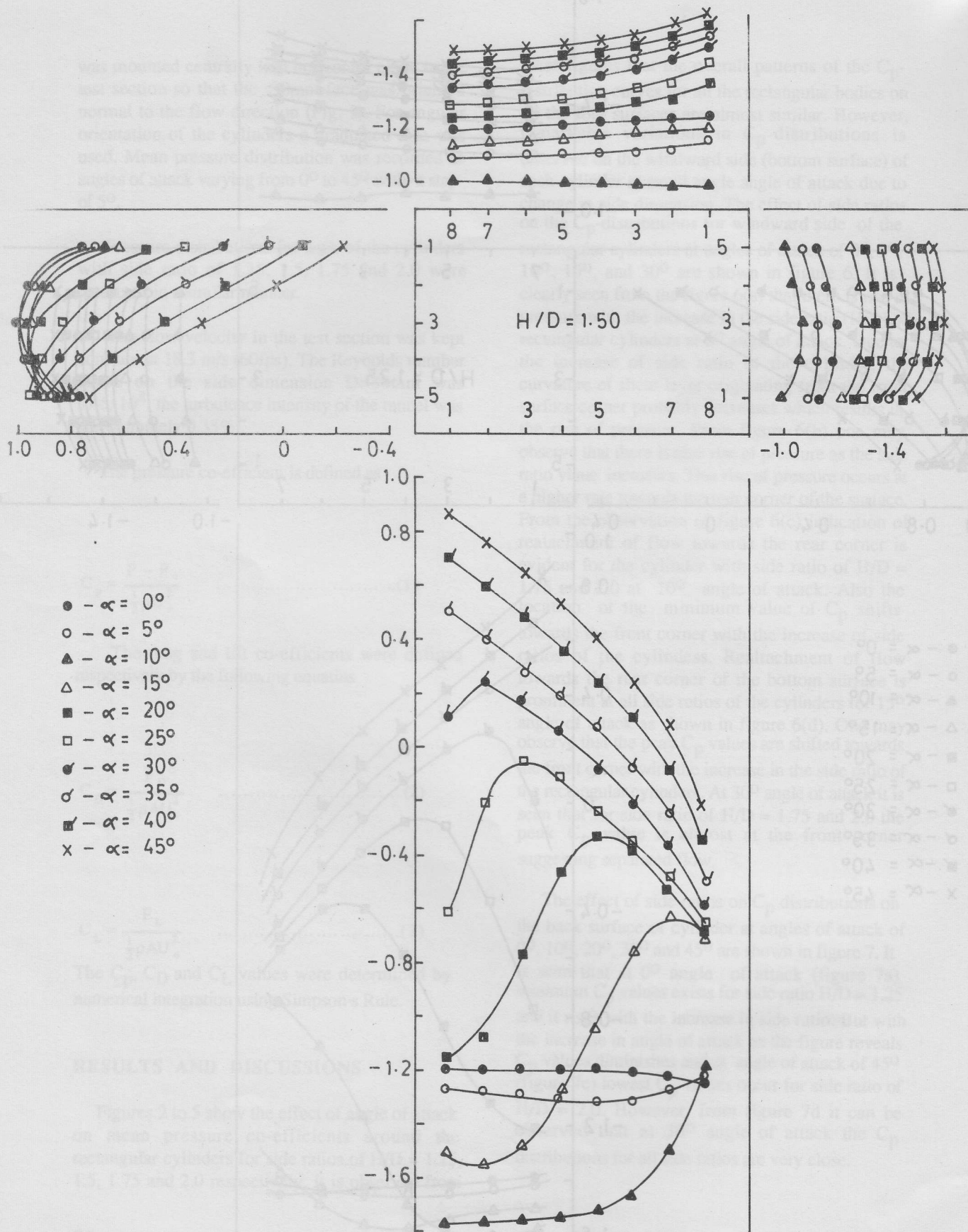


Figure 3: Effect of angle of attack on  $C_p$ -distribution at side ratio ( $H/D$ ) of 1.50.



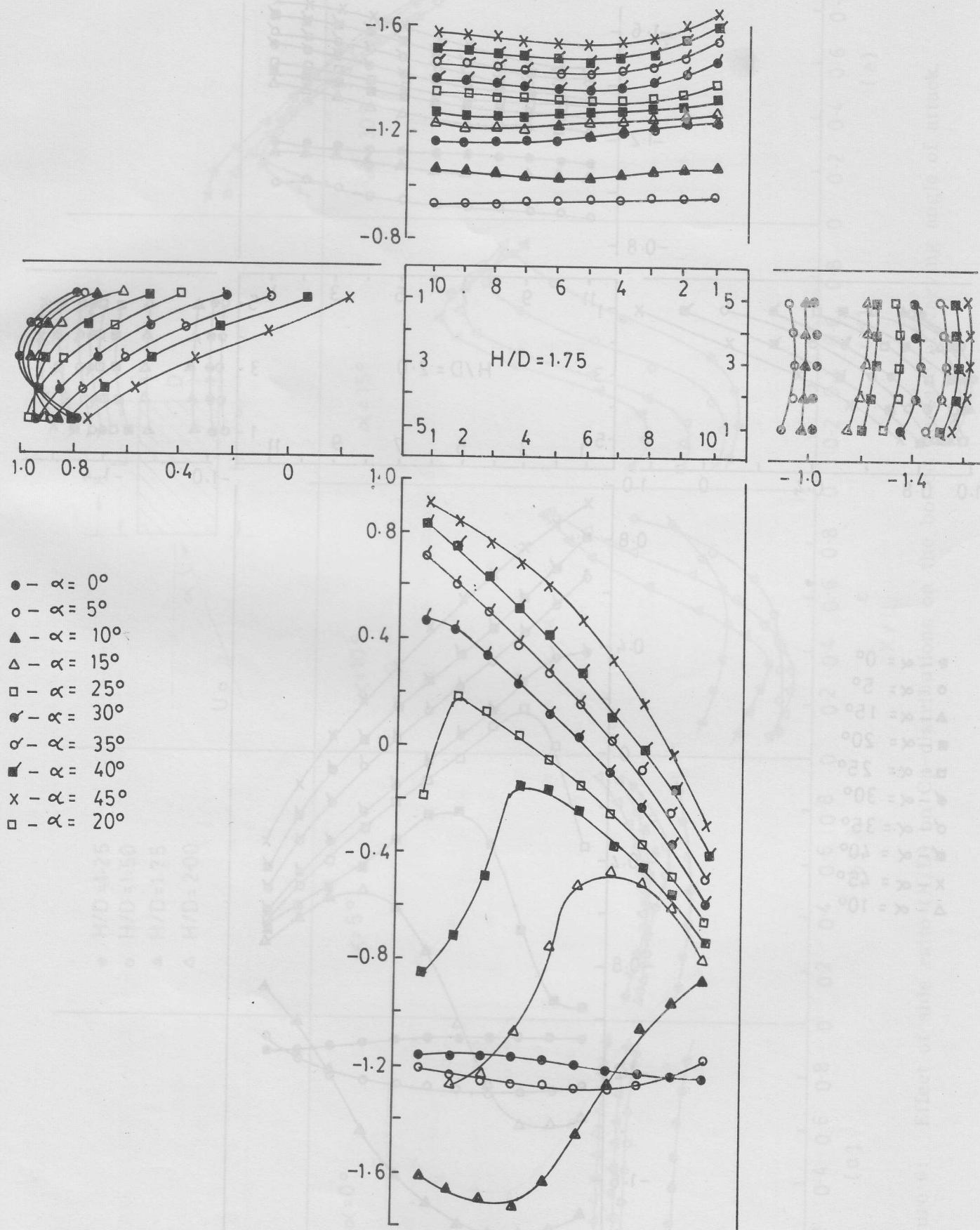
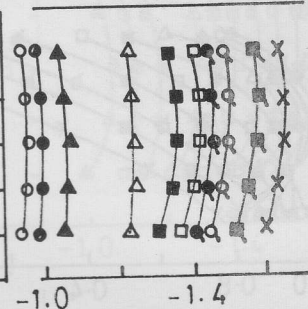
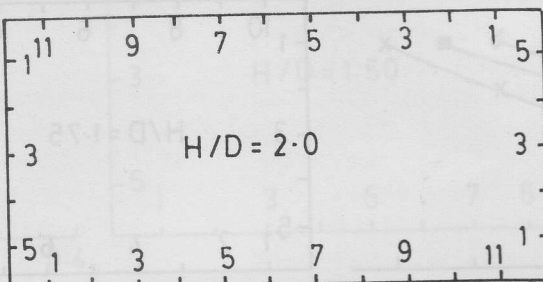
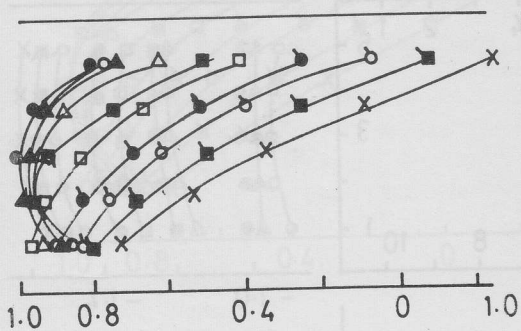
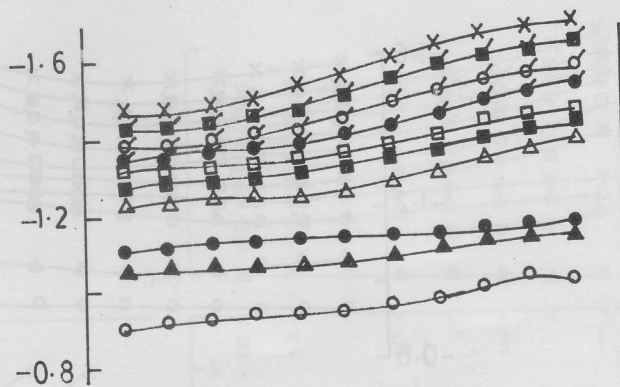


Figure 4: Effect of angle of attack ( $\alpha$ ) on  $C_p$ -distributions at side ratio ( $H/D$ ) of 1.75.



- -  $\alpha = 0^\circ$
- -  $\alpha = 5^\circ$
- ▲ -  $\alpha = 15^\circ$
- -  $\alpha = 20^\circ$
- -  $\alpha = 25^\circ$
- ◐ -  $\alpha = 30^\circ$
- ◑ -  $\alpha = 35^\circ$
- ◒ -  $\alpha = 40^\circ$
- × -  $\alpha = 45^\circ$
- △ -  $\alpha = 10^\circ$

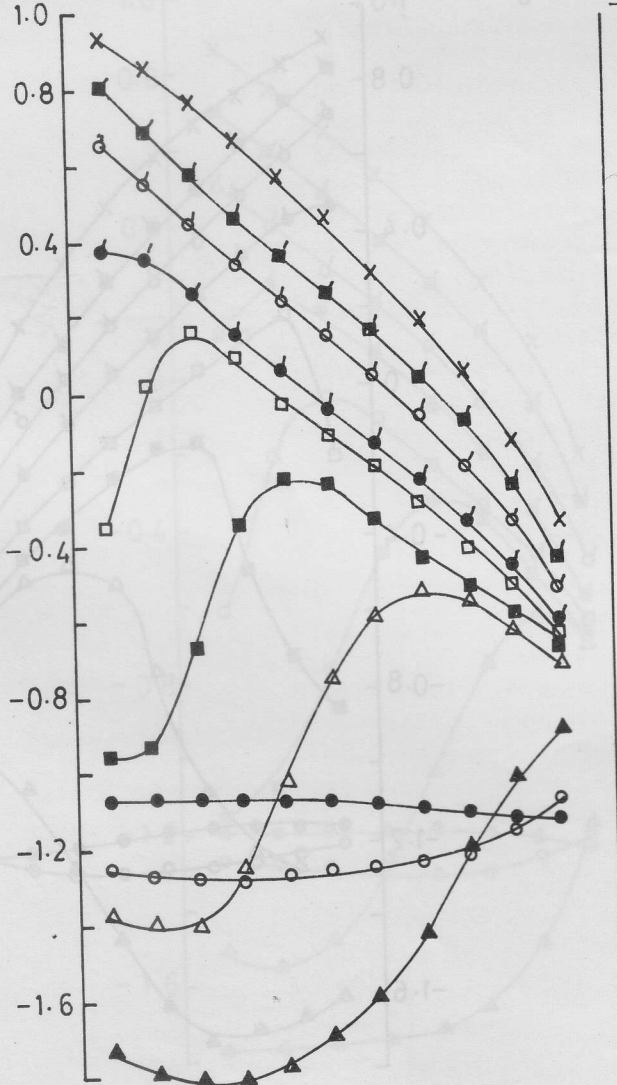


Figure 1. Velocity profiles at various angles of attack ( $\alpha$ ) on  $cn$ -distributions at  $H/D = 2.0$ .

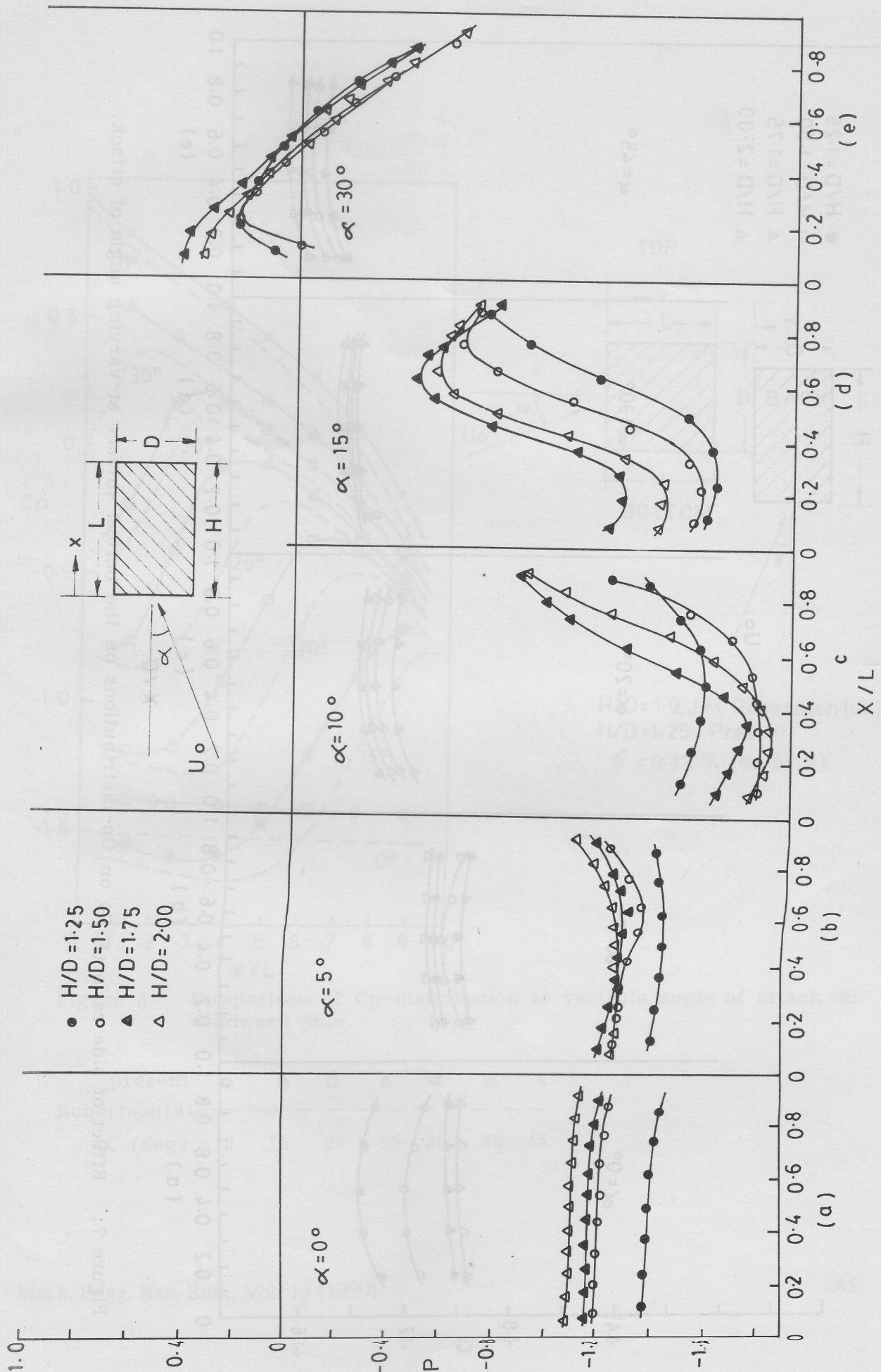


Figure 6: Effect of side ratio (H/D) on Cp-distributions on the bottom surface at varying angle of attack.



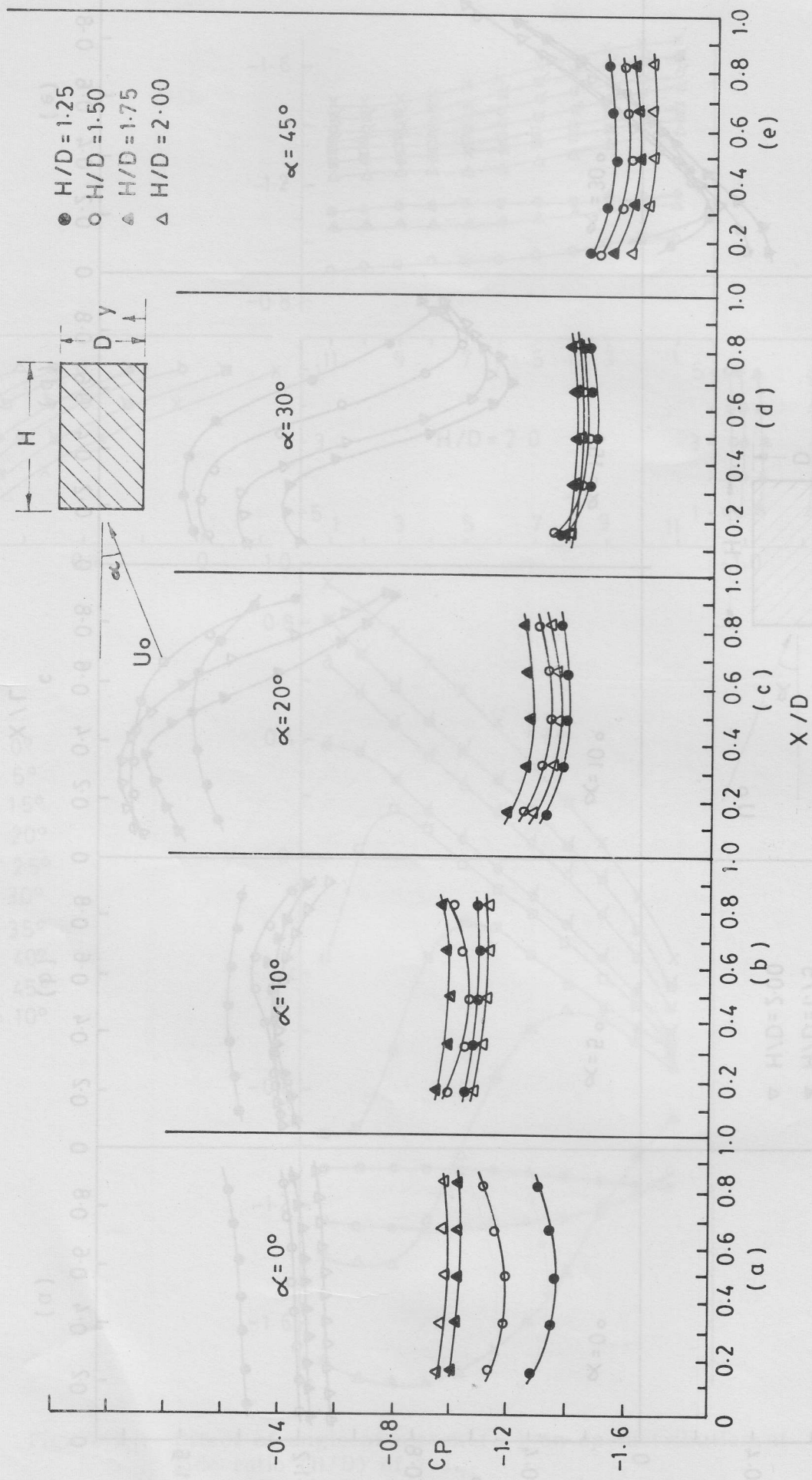
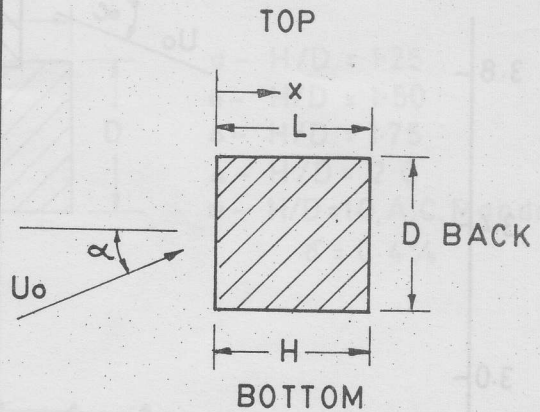
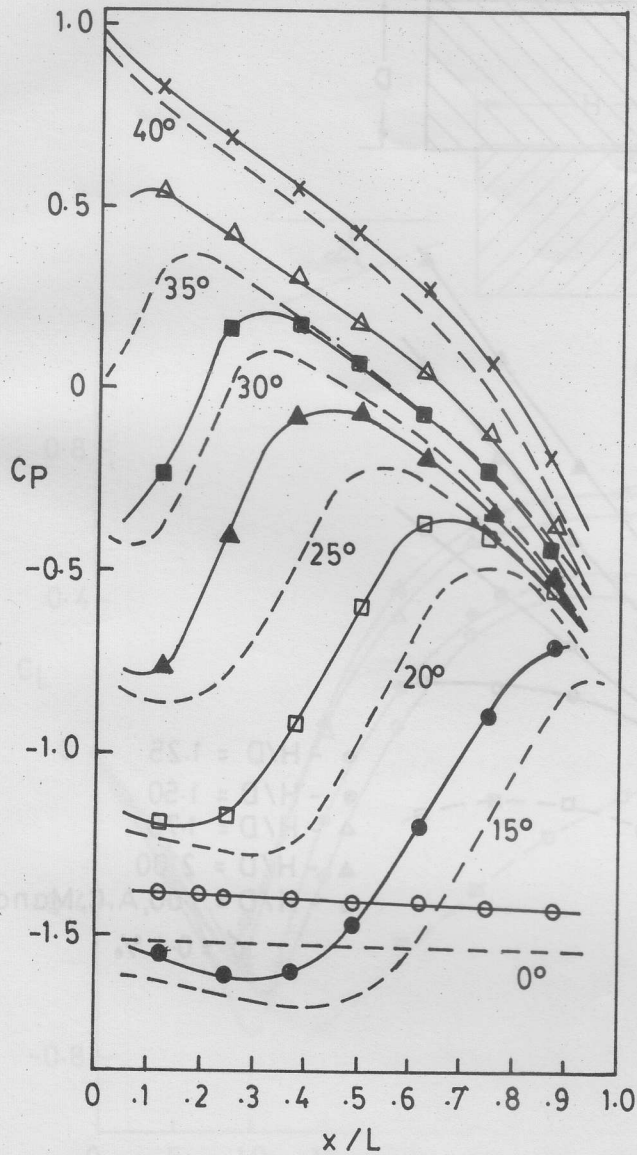


Figure 7: Effect of side ratio (H/D) on  $C_p$ -distributions on the bottom surface at varying angle of attack.



$H/D = 1.0$ , J.M. Roberston [41]  
 $H/D = 1.25$ , Present  
 $\delta = 0.33\%$  (for both)

Figure 8: Comparison of  $C_p$ -distribution at variable angle of attack on windward side.

present: ○ ● □ ▲ ■ △ ×  
 Robertson[41]: - - - - -  
 $\alpha$  (deg) : 0 15 20 25 30 35 45

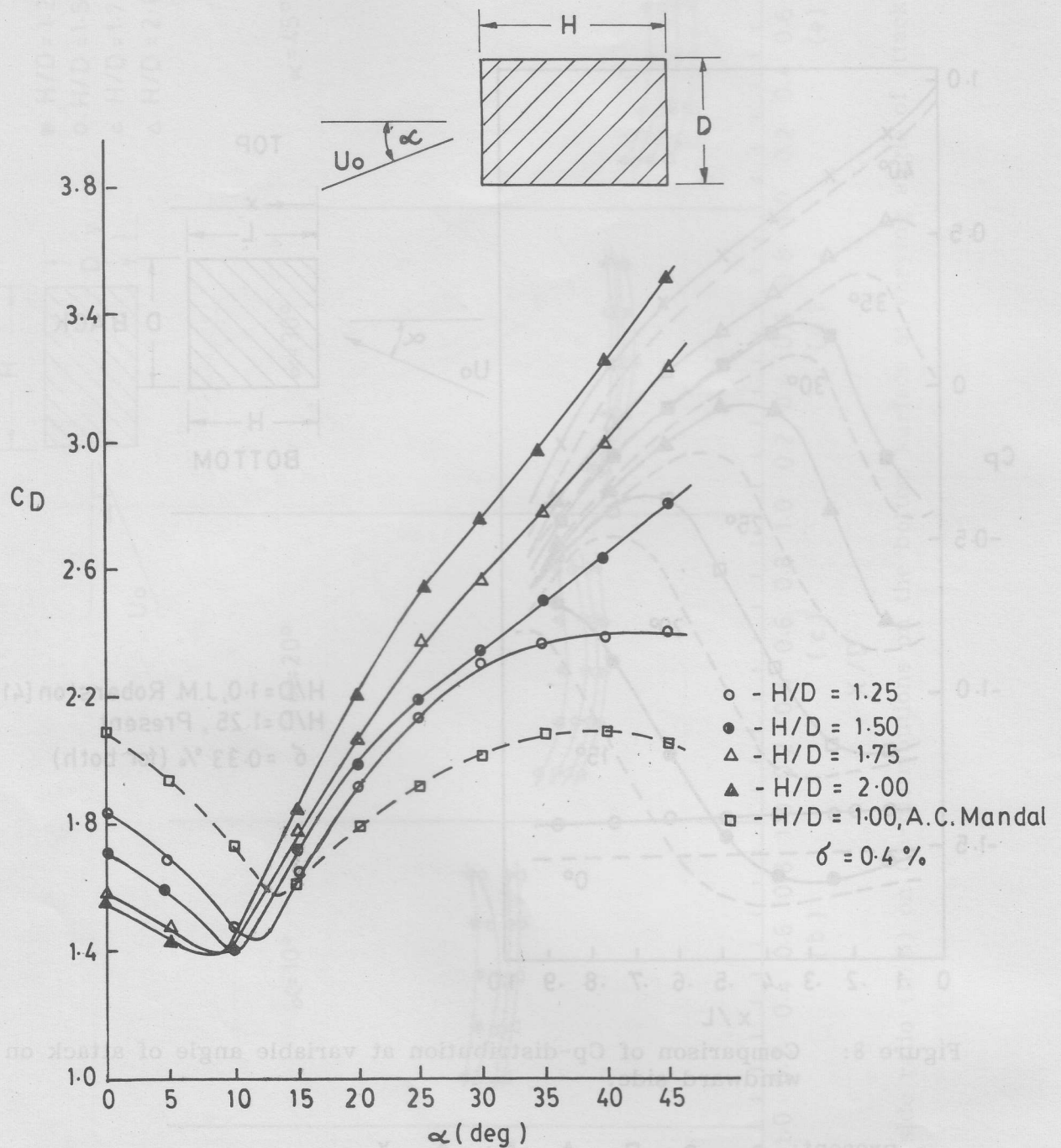


Figure 9: variation of drag coefficient ( $C_D$ ) with angle of attack ( $\alpha$ ) for different side ratios ( $H/D$ ).



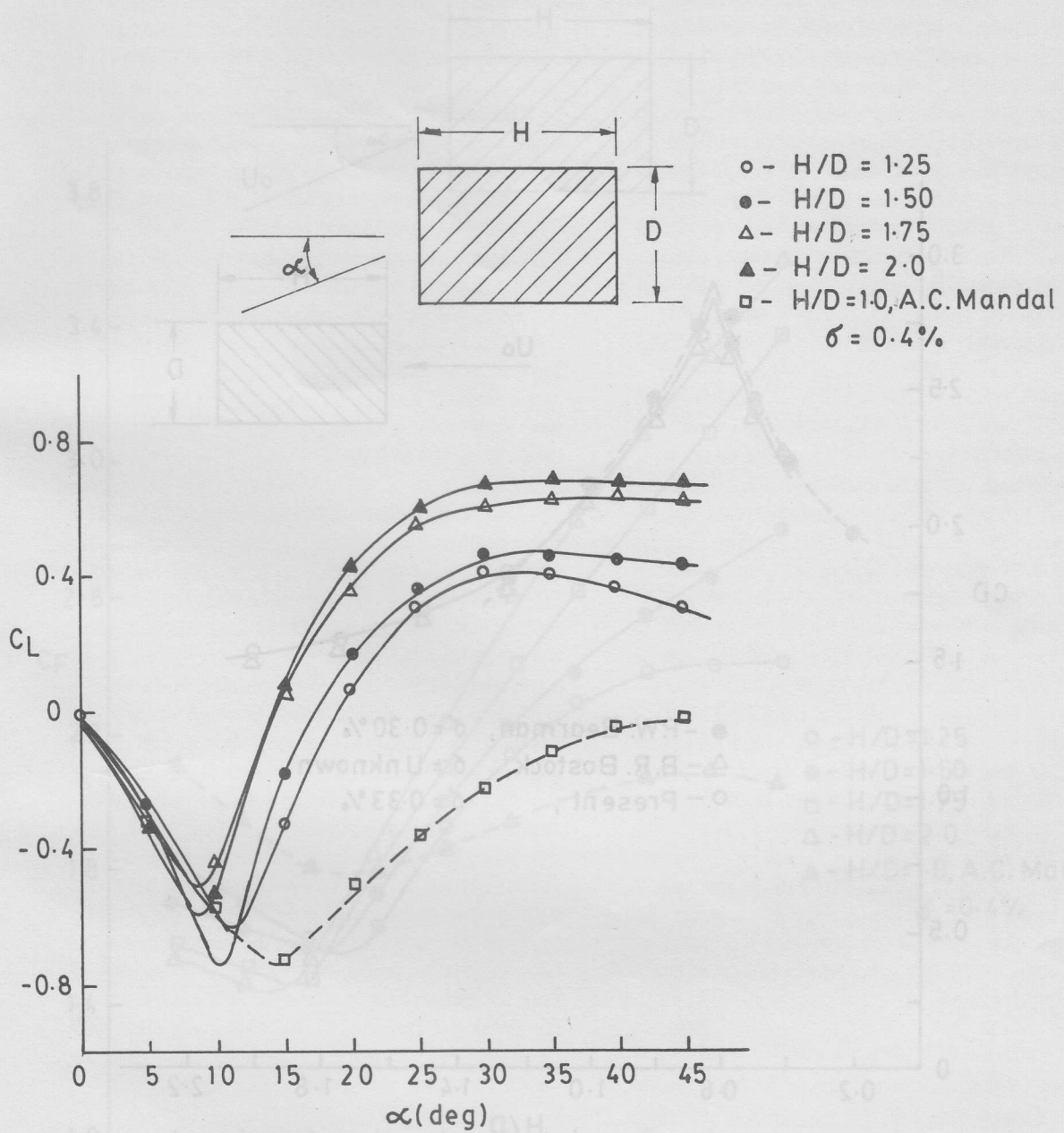


Figure 10: Variation of lift coefficient ( $C_L$ ) with angle of attack ( $\alpha$ ) for different side ratios ( $H/D$ ).

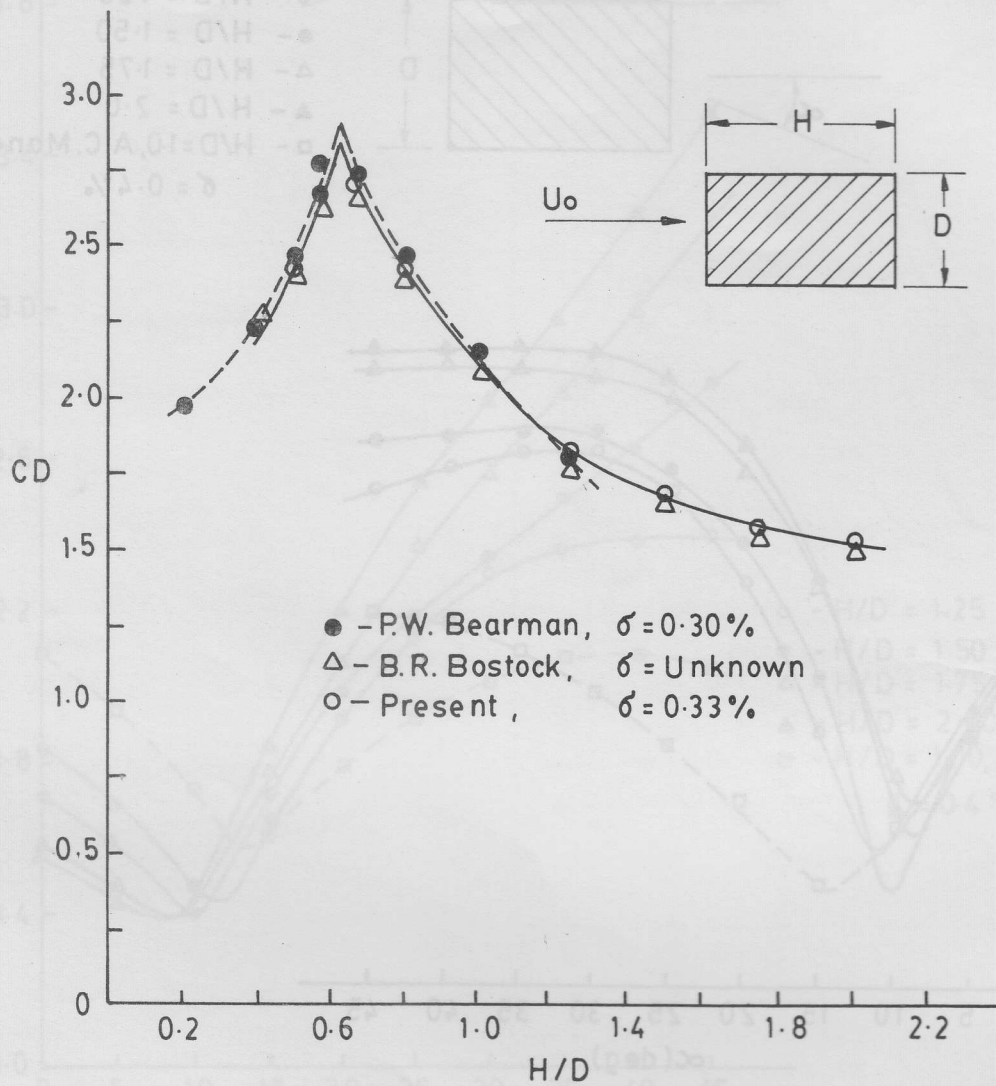


Figure 11: variation of drag coefficients with side ratios at angle of attack of  $0^\circ$ .

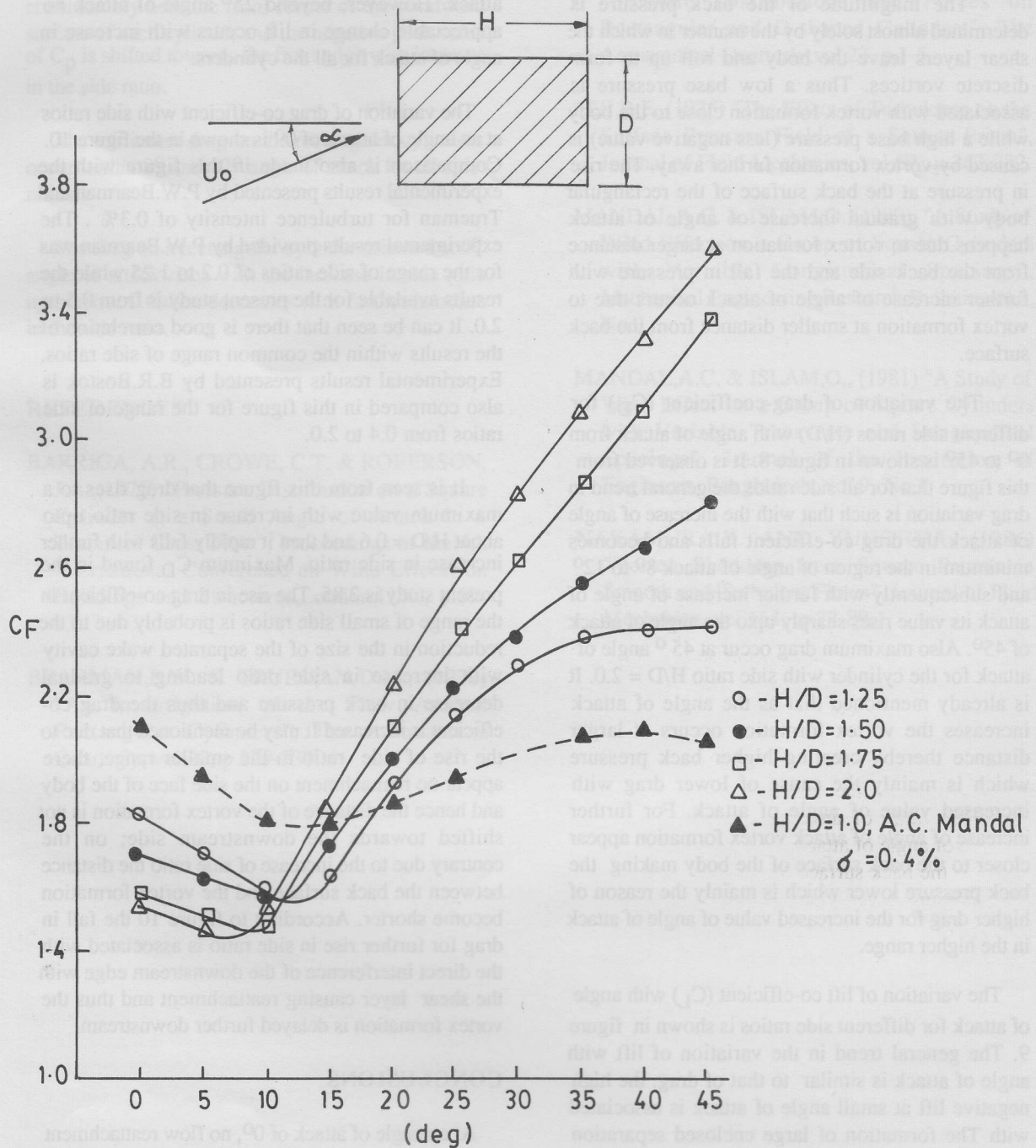


Figure 12: Variation of total force co-efficient ( $C_F$ ) with angle of attack ( $\alpha$ ) for different side ratios ( $H/D$ ).



The magnitude of the back pressure is determined almost solely by the manner in which the shear layers leave the body and roll up to form discrete vortices. Thus a low base pressure is associated with vortex formation close to the body while a high base pressure (less negative value) is caused by vortex formation further away. The rise in pressure at the back surface of the rectangular body with gradual increase of angle of attack happens due to vortex formation at larger distance from the back side and the fall in pressure with further increase of angle of attack occurs due to vortex formation at smaller distance from the back surface.

The variation of drag-coefficient ( $C_D$ ) for different side ratios ( $H/D$ ) with angle of attack from  $0^\circ$  to  $45^\circ$  is shown in figure 8. It is observed from this figure that for all side ratios the general trend in drag variation is such that with the increase of angle of attack the drag co-efficient falls and becomes minimum in the region of angle of attack  $8^\circ$  to  $12^\circ$  and subsequently with further increase of angle of attack its value rises sharply upto the angle of attack of  $45^\circ$ . Also maximum drag occur at  $45^\circ$  angle of attack for the cylinder with side ratio  $H/D = 2.0$ . It is already mentioned that as the angle of attack increases the vortex formation occurs at larger distance thereby creating higher back pressure which is mainly the cause of lower drag with increased value of angle of attack. For further increase of angle of attack vortex formation appear closer to the back surface of the body making the back pressure lower which is mainly the reason of higher drag for the increased value of angle of attack in the higher range.

The variation of lift co-efficient ( $C_L$ ) with angle of attack for different side ratios is shown in figure 9. The general trend in the variation of lift with angle of attack is similar to that of drag. the high negative lift at small angle of attack is associated with The formation of large enclosed separation bubble on the bottom surface of the cylinder which caused higher local suction than those on the top surface. As mentioned earlier the reattachment point on the bottom surface shifts towards the front corner with increase in the angle of attack thereby reducing the size of the separation bubble. This results in rise of lift co-efficient for further increase in angle of

attack. However, beyond  $25^\circ$  angle of attack no appreciable change in lift occurs with increase in angle of attack for all the cylinders.

The variation of drag co-efficient with side ratios at an angle of attack of  $0^\circ$  is shown in the figure 10. Comparison is also made in this figure with the experimental results presented by P.W.Bearman and Trueman for turbulence intensity of 0.3% . The experimental results provided by P.W.Bearman was for the range of side ratios of 0.2 to 1.25 while the results available for the present study is from 0.5 to 2.0. It can be seen that there is good correlation of the results within the common range of side ratios. Experimental results presented by B.R.Bostok is also compared in this figure for the range of side ratios from 0.4 to 2.0.

It is seen from this figure that drag rises to a maximum value with increase in side ratio upto about  $H/D = 0.6$  and then it rapidly falls with further increase in side ratio. Maximum  $C_D$  found in the present study is 2.85. The rise in drag co-efficient in the range of small side ratios is probably due to the reduction in the size of the separated wake cavity with increase in side ratio leading to gradual decrease in back pressure and thus the drag co-efficient is increased. It may be mentioned that due to the rise of side ratio in the smaller range, there appear no reattachment on the side face of the body and hence the distance of the vortex formation is not shifted towards the downstream side; on the contrary due to the increase of side ratio the distance between the back surface and the vortex formation become shorter. According to figure 10 the fall in drag for further rise in side ratio is associated with the direct interference of the downstream edge with the shear layer causing reattachment and thus the vortex formation is delayed further downstream.

## CONCLUSIONS

At an angle of attack of  $0^\circ$ , no flow reattachment occurs on the surfaces of each isolated rectangular cylinder. However, the  $C_p$  values on the top, bottom and back surfaces rise with the increase in side ratio of the rectangular cylinders.

Flow reattachment commences at smaller angle of attack if the side ratio increases.

At small angle of attack the  $C_p$  value decreases considerably near the front corner of the windward surface of each cylinder and the negative peak value of  $C_p$  is shifted towards the front edge with increase in the side ratio.

The minimum drag on the rectangular cylinders occur within  $8^\circ$  and  $12^\circ$  angle of attack for all side ratios.

The drag on a rectangular cylinder oriented at  $0^\circ$  angle of attack rises with the increase in side ratio upto about 0.6, then decreases with further increase in the side ratio.

## REFERENCES

- BARRIGA, A.R., CROWE, C.T. & ROBERSON, J.A., (1975) "Pressure Distribution on a Square Cylinder at a Small Angle of Attack in a Turbulent Cross Flow", Proceedings of the 4th International Conference on Wind Effects on Buildings and Structures, London, U.K., p.89-93.
- BEARMAN, P.W. & TRUEMAN, D.M., (1972) "An Investigation of the Flow Around Rectangular Cylinders", The Aeronautical Quarterly, vol.23, p.229-237.
- BOSTOK, B.R. AND MAIR, W.A., (1972) "Pressure Distributions and Forces on Rectangular and D-shaped Cylinders", The Aeronautical Quarterly, vol.23, p.1-5.
- LEE, B.E., (1975) "The Effect of Turbulence on the Surface Pressure Field of a Square Prism", Journal of Fluid Mechanics, vol.69, p.263-282.
- MANDAL, A.C. & ISLAM, O., (1980) "A Study of Wind Effect on a Group of Square Cylinders with Variable Longitudinal Spacings", Mechanical Engineering Research Bulletin, vol.3, No.1,
- MANDAL, A.C. & ISLAM, O., (1981) "A Study of Wind Effect on a Group of Square Cylinders with Variable Transverse and Longitudinal Spacings", Journal of the Institution of Engineers, Bangladesh, vol.9, No.1,
- NAKAMURA, Y. AND YUJIOHYA, (1986) "Vortex Shedding from Square Prisms in Smooth and Turbulent Flows", Journal of Fluid Mechanics, vol.164, p.77-89.